



Fermi National Accelerator Laboratory

FERMILAB-Conf-99/310-E

KTeV

Observation of Direct-CP Violation

Yee Bob Hsiung
For the KTeV Collaboration

*Fermi National Accelerator Laboratory
P.O. Box 500, Batavia, Illinois 60510*

November 1999

Published Proceedings of the *OCPA Conference on Recent Advances and Cross-Century Outlooks in Physics*, Atlanta, Georgia, March 18-20, 1999

Disclaimer

This report was prepared as an account of work sponsored by an agency of the United States Government. Neither the United States Government nor any agency thereof, nor any of their employees, makes any warranty, expressed or implied, or assumes any legal liability or responsibility for the accuracy, completeness, or usefulness of any information, apparatus, product, or process disclosed, or represents that its use would not infringe privately owned rights. Reference herein to any specific commercial product, process, or service by trade name, trademark, manufacturer, or otherwise, does not necessarily constitute or imply its endorsement, recommendation, or favoring by the United States Government or any agency thereof. The views and opinions of authors expressed herein do not necessarily state or reflect those of the United States Government or any agency thereof.

Distribution

Approved for public release; further dissemination unlimited.

Copyright Notification

This manuscript has been authored by Universities Research Association, Inc. under contract No. DE-AC02-76CH03000 with the U.S. Department of Energy. The United States Government and the publisher, by accepting the article for publication, acknowledges that the United States Government retains a nonexclusive, paid-up, irrevocable, worldwide license to publish or reproduce the published form of this manuscript, or allow others to do so, for United States Government Purposes.

OBSERVATION OF DIRECT- CP VIOLATION

YEE BOB HSIUNG

Fermilab, P. O. Box 500, Batavia, IL 60510, USA

E-mail: hsiung@fnal.gov

(KTeV Collaboration: Arizona, Chicago, Colorado, Elmhurst, Fermilab, Osaka, Rice, Rutgers, UCLA, UCSD, Virginia and Wisconsin)

Using a subset of data collected in the 1996-97 fixed target run at Fermilab, we report the first preliminary measurement on the direct- CP violation from the KTeV experiment. The result is, $\epsilon'/\epsilon = (28.0 \pm 4.1) \times 10^{-4}$, nearly 7 standard deviations above zero obtained by a blind analysis. This establishes the long-sought “direct- CP violation” effect in the two-pion system of neutral kaon decays. The experimental technique, data analysis and systematic checks for this measurement are discussed and the comparison with other measurements is also presented.

1 Introduction

One of the long lasting puzzles in particle physics is the origin of the violation of CP symmetry in weak interactions, where C stands for the charge conjugation (exchange particle and anti-particle) and P stands for the parity (space inversion). Ever since the unexpected discovery¹ of CP violation in $K_L \rightarrow \pi\pi$ decays in 1964 (where the dominant effect is in the asymmetry of the $K^0 - \bar{K}^0$ mixing or admixture of wrong CP states in the K_S and K_L neutral kaons, parametrized by ϵ which is about 0.0023), there has been great interest in determining whether CP violation also occurs in the $K \rightarrow \pi\pi$ decay process itself, an effect referred to as “direct” CP Violation.² The “direct” CP Violation, parametrized by ϵ' , contributes differently to the rates of $K_L \rightarrow \pi^+\pi^-$ versus $K_L \rightarrow \pi^0\pi^0$ decays (relative to the corresponding K_S decays), and would be observed as a nonzero value in the ratio of $\text{Re}(\epsilon'/\epsilon)$.

Experimentally we measure the double ratio R ,

$$R = \frac{\Gamma(K_L \rightarrow \pi^+\pi^-)/\Gamma(K_S \rightarrow \pi^+\pi^-)}{\Gamma(K_L \rightarrow \pi^0\pi^0)/\Gamma(K_S \rightarrow \pi^0\pi^0)} \approx 1 + 6\text{Re}(\epsilon'/\epsilon). \quad (1)$$

The standard Cabbibo-Kobayashi-Maskawa (CKM) model³ accomodates CP violation with a complex phase in the quark mixing matrix, but the calculations of $\text{Re}(\epsilon'/\epsilon)$ depend on several input parameters and on the method used to estimate the hadronic matrix elements. Most recent estimates^{4, 5} have given non-zero values slightly below 10^{-3} ; however, another group⁶ gives a somewhat larger range of estimates. Alternatively, a “superweak” interaction⁷ could produce the observed CP -violating mixing effect (ϵ) but would give

$\text{Re}(\epsilon'/\epsilon) = 0$. Therefore, a non-zero value of $\text{Re}(\epsilon'/\epsilon)$ measurement rules out the possibility that a superweak interaction is the sole source of CP violation, and would establish the “direct” CP violation from the decay process itself.

The two most recent measurements of $\text{Re}(\epsilon'/\epsilon)$ from Fermilab-E731⁸ and CERN-NA31⁹ were

$$\text{Re}(\epsilon'/\epsilon) = (7.4 \pm 5.9) \times 10^{-4}, \quad (E731) \quad (2)$$

$$\text{Re}(\epsilon'/\epsilon) = (23.0 \pm 6.5) \times 10^{-4}, \quad (NA31) \quad (3)$$

which gave inconclusive interpretations between standard model and superweak CP -violation. New experiments have been constructed at Fermilab, CERN and Frascati to measure $\text{Re}(\epsilon'/\epsilon)$ with a precision of $(1 \sim 2) \times 10^{-4}$ for the search of “direct” CP violation and determining its magnitude.

We report here a new measurement of $\text{Re}(\epsilon'/\epsilon)$ based on 23% of the data collected by the KTeV experiment (E832) during 1996-97 run at Fermilab.

2 KTeV Experiment and Double Beam Method

The KTeV experiment was designed to improve on the previous experiments and ultimately to have the sensitivity to establish direct CP violation if $\text{Re}(\epsilon'/\epsilon)$ is on the order of 10^{-3} . The experimental technique is the same as in E731,¹⁰ and differs from NA31¹¹ in two key ways. First it uses double kaon beams from a single target to enable the simultaneous collection of K_L and K_S decays to minimize the systematics due to time variation of beam flux and detector inefficiencies. Second, it uses a precision magnetic spectrometer to minimize backgrounds in the $\pi^+\pi^-$ samples and to allow *in situ* calibration of the calorimeter with electrons. A high precision electromagnetic calorimeter, Cesium Iodide (CsI) crystal array, is used for $\pi^0\pi^0$ reconstruction and better background suppression. A new beamline was constructed for KTeV with cleaner beam collimation and improved muon sweeping. While the method of producing a K_S beam (by passing a K_L beam through a “regenerator”) is also the same as E731, the KTeV regenerator is made of scintillator and is fully active to reduce the scattered background to the coherently regenerated K_S .

The KTeV detector is shown in Fig. 1. Two beams (called “regenerator” and “vacuum”) enter the evacuated decay volume, with the main detector elements located downstream. The regenerator alternates sides once per accelerator cycle to minimize the effect of any left-right beam or detector asymmetry. A movable “shadow absorber” far upstream attenuates the kaon beam incident on the regenerator. To measure the double ratio of decay rates for $\text{Re}(\epsilon'/\epsilon)$, we need understand the difference between the acceptances for K_S versus K_L decays to each $\pi\pi$ final state. Event reconstruction and selection are done

with identical criteria for decays in either beam, so the principle difference between the K_S and K_L data samples is in the decay vertex distributions, shown in Fig. 2 as a function of Z , the distance from the target. Therefore, the most crucial requirement of measuring $\text{Re}(\epsilon'/\epsilon)$ with this technique is a precise understanding of the Z -dependence of the detector acceptance. In contrast, NA31 uses a movable K_S target train to match the K_S and K_L decay Z distributions, causing the acceptance to nearly cancel.

In the vacuum beam, the acceptance for decays upstream of $Z = 122\text{ m}$ is limited by a lead-scintillator counter, “mask-anti” (MA), with two square holes 50% larger than the beams. In the regenerator beam, the beginning of the decay region is sharply defined by a thin lead-scintillator module at the downstream end of the 1.7 m long regenerator.

The spectrometer consists of four drift chambers, each with two horizontal and two vertical planes of sense wires, and a large dipole magnet with 412 MeV/c transverse momentum kick for the momentum measurement of charged particles. The typical position resolution is 110 μm for the chamber and the momentum resolution is 0.4% at the mean pion momentum of 36 GeV/c .

The electromagnetic calorimeter consists of 3100 blocks of pure CsI in a square array 1.9 m on a side and 50 cm deep. Two 15 cm square holes allow passage of the neutral beams through the calorimeter. The calorimeter was calibrated using 190 million momentum-analyzed electrons from $K_L \rightarrow \pi e \nu$ decays collected during the normal running. The average energy resolution for photons from $\pi^0\pi^0$ is 0.7% with a mean photon energy of 19 GeV .

The inner aperture at the CsI is defined by a tungsten-scintillator counter (CA) around each beam hole. In addition, there are ten lead-scintillator “photon veto” counters to detect particles escaping from the decay volume or missing the CsI, in order to suppress the major $K_L \rightarrow 3\pi^0$ background to the CP -violated $\pi^0\pi^0$ signal mode.

The charged mode (for $\pi^+\pi^-$, $Ke3$) trigger is based on a scintillator hodoscope located just upstream of the CsI calorimeter and requirements on the number and pattern of hits in the drift chambers. The neutral mode trigger is based on a fast energy sum from the calorimeter and a hardware cluster finding processor (e.g. for $\pi^0\pi^0$ it must find 4 or 5 clusters of energy in the CsI). Additional fast veto signals from the regenerator, a subset of photon vetoes and a downstream muon veto hodoscope located behind 4 m of steel are also used in the trigger to keep the trigger rate at a manageable level. After readout, a CPU-based “Level 3 filter” reconstructs events and applies loose kinematic cuts to select $\pi^+\pi^-$ and $\pi^0\pi^0$ candidates. Large samples of $K_L \rightarrow \pi e \nu$ and $K_L \rightarrow 3\pi^0$ decays are recorded for detector calibration and acceptance studies.

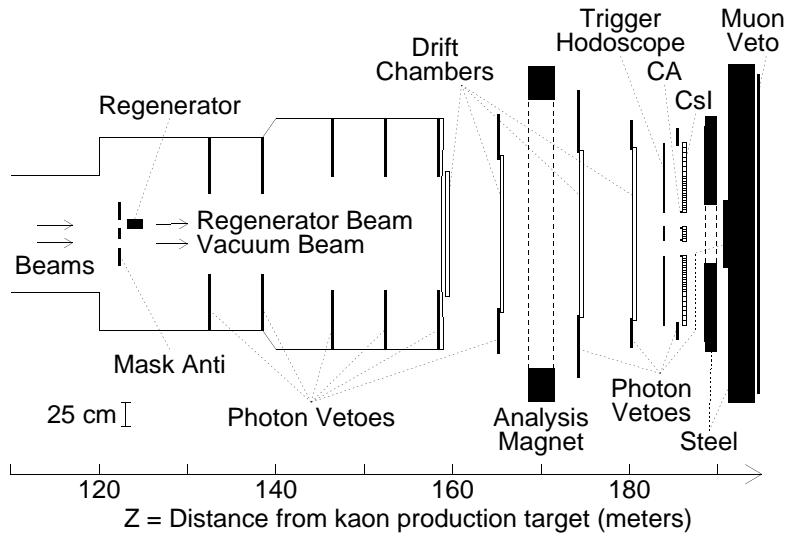


Figure 1: Plan view of the KTeV apparatus with double kaon beam as configured to measure $\text{Re}(\epsilon'/\epsilon)$. The evacuated decay volume ends with a thin vacuum window at $Z = 159$ m. The label “CsI” indicates the electromagnetic calorimeter.

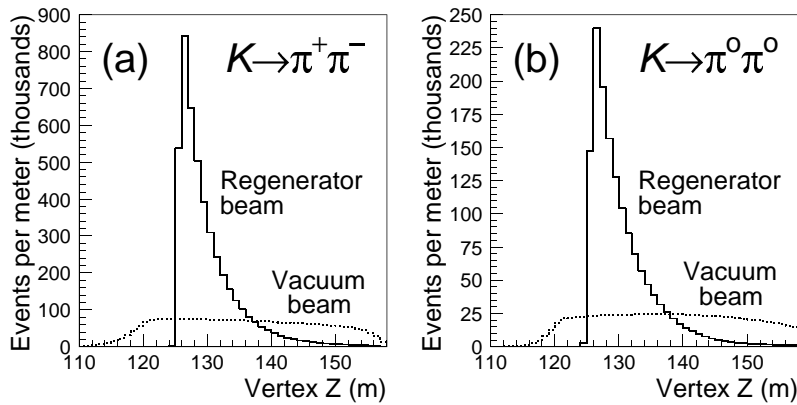


Figure 2: Decay vertex distributions for the (a) $K \rightarrow \pi^+ \pi^-$ and (b) $K \rightarrow \pi^0 \pi^0$ decay modes, showing the difference between the “regenerator” (K_S) and “vacuum” (K_L) beams.

In addition, an “accidental” trigger is formed by using scintillation counters near 90° to the target to randomly record the underlying activity in the KTeV detector with the same instantaneous rate as the physics data for study.

The $\pi^0\pi^0$ samples in this analysis were collected in 1996, while $\pi^+\pi^-$ samples were from the first 18 days of data in 1997. The 1996 $\pi^+\pi^-$ samples are analyzed but not used for this result because of a large Level 3 tracking inefficiency (about 22% loss) from an unanticipated drift chamber effect which sometimes delayed a hit by 20 ns or more. The inefficiency was nearly the same for both beams but still would have led to a larger systematic error. The Level 3 software was modified for 1997 run to allow for this effect, resulting in an inefficiency of less than 0.1% and reduced systematics. The construction of a double ratio (Eq. 1) allows us to use data from different time periods with small systematics.

3 ϵ'/ϵ Analysis

Event reconstruction and selection are done with identical cuts and criteria for decays in either beam to minimize the systematics. For the selection of $\pi^+\pi^-$ candidates, each pion is required to have a momentum $p_\pi > 8 \text{ GeV}/c$ and to deposit less than 85% of its energy in the CsI calorimeter. Cuts are also made on the distance from each pion to the edges of the detectors, and on the separation distance between the two pions at the chambers and calorimeter to avoid poorly reconstructed event topology and to cleanly define the acceptance. The $\pi^+\pi^-$ invariant mass is required to be between 488 and 508 MeV/c^2 (where the mass resolution is about 1.6 MeV/c^2) and the square of the transverse momentum of the $\pi^+\pi^-$ system relative to the initial kaon trajectory from target, p_T^2 , is required to be less than 250 MeV^2/c^2 .

The $\pi^0\pi^0$ candidates are reconstructed from four-photon events by choosing the photon pairing combination which is most consistent with the hypothesis of two π^0 decays at a common kaon decay vertex. Each photon is required to have an energy $E_\gamma > 3 \text{ GeV}$ and to be at least 5 cm away from the outer edge of the CsI and 7.5 cm from any other photon. The $\pi^0\pi^0$ invariant mass is required to be between 490 and 505 MeV/c^2 , where the mass resolution is about 1.5 MeV/c^2 .

The initial kaon trajectory is unknown, so the only available indicator of kaon scattering is the position of the energy centroid of the four photons at the CsI. This is used to calculate a box “ring number”, defined as four times the square of the larger normal distance (either horizontal or vertical), in unit of cm , from the centroid to the center of the closer beam. Its value is required to be less than 110, which selects events with energy centroid lying within a

square region of area 110 cm^2 centered on each beam.

In both $\pi^+\pi^-$ and $\pi^0\pi^0$ analyses, cuts are made on energy deposits in the MA, photon veto counters and regenerator. The final samples consist of events with $110 < Z < 158 \text{ m}$ and $40 < E_K < 160 \text{ GeV}$.

A detailed Monte Carlo (MC) simulation is used to determine the detector acceptance and to evaluate backgrounds. The simulation models kaon production and regeneration to generate decays with the same energy E_K and decay vertex Z distributions as the data. The decay products are traced through the KTeV detector, allowing for electromagnetic interactions with detector material and pion decay. The acceptance is largely determined by the geometry of the detector and by geometric analysis cuts. Simulation of the detector response is also included to understand the reconstruction biases. High statistics $\pi e\nu$ and $3\pi^0$ data samples are used to check or tune various aspects of the detector geometry and simulation. To reproduce the biases due to underlying activity in the detector, an event from the “accidental” trigger is overlaid on top of each simulated decay; the net effect on $\text{Re}(\epsilon'/\epsilon)$ is of order 10^{-4} .

Backgrounds to the $\pi^+\pi^-$ samples are determined by using sidebands in the mass and p_T^2 distributions to normalize MC predictions from various background processes. Figure 3 (a) and (b) show that the p_T^2 distributions for data are well described by the sum of coherent $\pi\pi$ MC and total background MC. Semileptonic $K_L \rightarrow \pi e\nu$ and $K_L \rightarrow \pi\mu\nu$ decays, with the electron or muon misidentified as a pion, contribute 0.069% mainly to the vacuum beam. The dominant regenerator-beam background (0.072%) is from kaons which scatter in the regenerator before decaying to $\pi^+\pi^-$. Kaons which scatter in the final beam-defining collimator contribute an additional 0.014% to each beam. Each type of scattering is parametrized using the $\pi^+\pi^-$ data of the same running period and incorporated into the MC simulation.

Background levels are much larger for the $\pi^0\pi^0$ samples since the ring-number variable is not as effective as p_T^2 at identifying scattered kaons and detecting “crossover” scattering from the regenerator into the vacuum beam. Ring-number distributions are shown in Fig. 3 (c) and (d). The upturn under the peak in (c) is due to $K_L \rightarrow 3\pi^0$ decays with lost and/or overlapping photons; it is determined, using mass sidebands, to contribute a background of 0.27% mainly to the vacuum beam. Ring-number sidebands are used to normalize MC distributions from kaons that scatter in the regenerator or collimator before decaying to $\pi^0\pi^0$. The vacuum (regenerator) beam background includes 0.30% (1.07%) from regenerator scattering and 0.16% (0.14%) from collimator scattering. Pairs of π^0 's produced by hadronic interactions in the regenerator contribute a small additional background of 0.01% in that beam.

After background subtraction, the net yields are 2.607M $\pi^+\pi^-$ events in

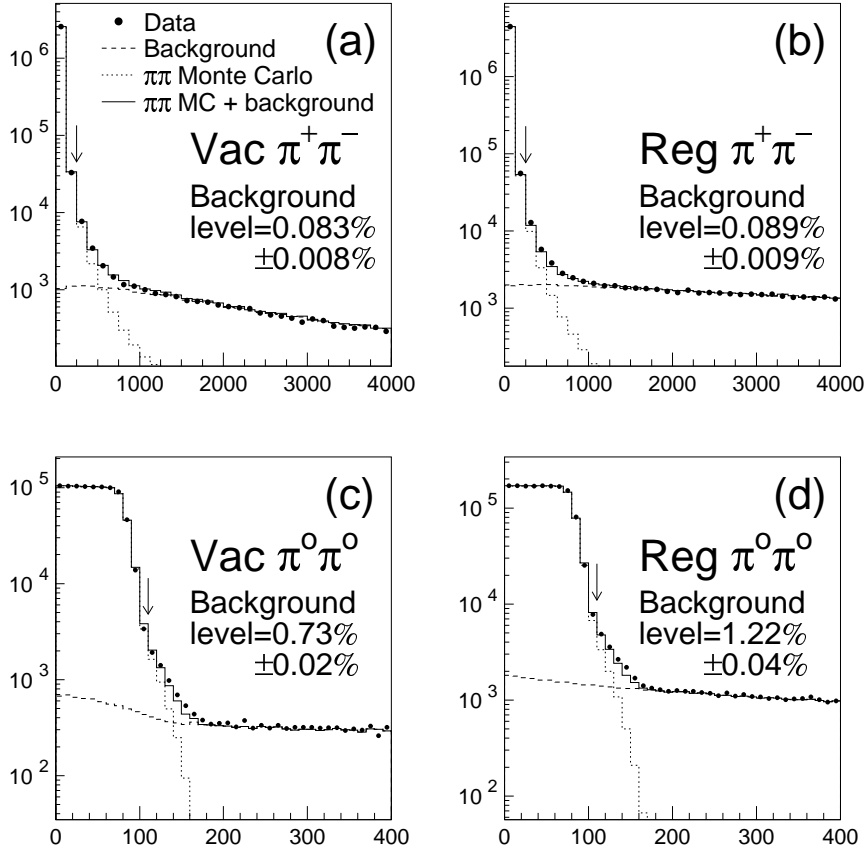


Figure 3: Distributions of p_T^2 for the $\pi^+\pi^-$ samples and ring number for the $\pi^0\pi^0$ samples. Total background levels and uncertainties (dominated by systematics) are given for the samples passing the analysis cuts (arrows).

the vacuum beam, 4.516M $\pi^+\pi^-$ in the regenerator beam, 862K $\pi^0\pi^0$ in the vacuum beam and 1.434M $\pi^0\pi^0$ in the regenerator beam.

4 ϵ'/ϵ Fits

$\text{Re}(\epsilon'/\epsilon)$ is extracted from the background-subtracted data using a fitting program which analytically calculates regeneration and decay distributions accounting for $K_S - K_L$ interference. The acceptance correction is applied, and the resulting prediction for each decay mode is integrated over Z and compared to data in 10 GeV bins of kaon energy. CPT symmetry is assumed, and the values of $K_S - K_L$ mass difference (Δm) and K_S lifetime (τ_S) are fixed to PDG values.¹² The regeneration amplitude is floated in the fit, but constrained to have a power law dependence on kaon energy, with the phase determined by analyticity.^{10, 13} The kaon energy distribution are allowed to float for $\pi^+\pi^-$ and $\pi^0\pi^0$ modes in each energy bin (24 fit parameters in all).

Fitting was done “blind”, by hiding the value of $\text{Re}(\epsilon'/\epsilon)$ with an unknown offset, until after the analysis and systematic error evaluation were finalized. The final result is $\text{Re}(\epsilon'/\epsilon) = (28.0 \pm 3.0) \times 10^{-4}$, where the error is statistical only. The fit χ^2 is 30 for 21 degrees of freedom.

5 Systematics and Checks

Only biases which affect the K_L and K_S samples differently will lead to systematic errors on $\text{Re}(\epsilon'/\epsilon)$. Possible sources are divided into four classes: (1) data collection inefficiencies; (2) biases in event reconstruction, sample selection, and background subtraction; (3) misunderstanding of the detector acceptance; and (4) uncertainties in kaon flux and physics parameters. Table 1 summarizes all of the estimated contributions; only those that are large or require special explanation will be discussed below.

Two of the largest uncertainties in the second class are related to the measurement of photon energies by the calorimeter. A systematic shift in measured energies can shift the reconstructed Z vertex and E_K distributions for the $\pi^0\pi^0$ sample and thus can bias $\text{Re}(\epsilon'/\epsilon)$, mainly by moving K_L events past the fiducial Z cut at 158 m . After calibrating the calorimeter with electrons (and allowing for a small expected electron-photon difference), a final energy scale correction for photons of -0.125% is determined by matching the sharp turn-on of the $\pi^0\pi^0$ Z distribution at the regenerator edge between data and MC. After making this correction, a check using π^0 pairs produced by hadronic interactions in the vacuum window reveals a Z mismatch of 2 cm at the downstream end of the decay region, leading to a systematic error of

Table 1: Systematic uncertainties on $\text{Re}(\epsilon'/\epsilon)$.

Source of Uncertainty	Uncertainty ($\times 10^{-4}$)	
	$\pi^+\pi^-$	$\pi^0\pi^0$
1. Data Collection		
Trigger and Level 3 filter	0.5	0.3
2. Reconstruction, Selection, Backgrounds		
Energy scale	0.1	0.7
Calorimeter nonlinearity	...	0.6
Detector calibration, alignment	0.3	0.4
Analysis cut variations	0.6	0.8
Background subtraction	0.2	0.8
3. Detector Acceptance		
Limiting apertures	0.3	0.5
Detector resolution	0.4	<0.1
Drift chamber simulation	0.6	...
Z dependence of acceptance	1.6	0.7
Monte Carlo statistics	0.5	0.9
4. Kaon Flux and Physics Parameters		
Regenerator-beam attenuation:		
1996 versus 1997		0.2
Energy dependence		0.2
$\Delta m, \tau_S$, regeneration phase		0.2
TOTAL		2.8

0.7×10^{-4} on $\text{Re}(\epsilon'/\epsilon)$. Residual nonlinearities in the calorimeter response contribute an additional error of 0.6×10^{-4} .

We assign systematic errors based on the dependence of the measured value of $\text{Re}(\epsilon'/\epsilon)$ on variations of key analysis cuts, in particular the p_T^2 cut for $\pi^+\pi^-$ and the ring-number and photon quality cuts for $\pi^0\pi^0$. No significant dependence is observed on other analysis cuts.

The accuracy of the background determination for the $\pi^0\pi^0$ samples depends on our understanding of kaon scattering in the regenerator and collimator. We consider several variations in the procedure for determining the scattering distributions from the $K \rightarrow \pi^+\pi^-$ data; these affect the shapes of the background MC ring-number distributions, but the sideband normalization procedure limits the impact on $\text{Re}(\epsilon'/\epsilon)$ ($\leq 0.8 \times 10^{-4}$).

The third class of systematics, related to detector acceptance, contributes the most to the total systematic error. Many potential detector modeling problems would affect the acceptance as a function of Z , so a crucial check of our understanding of the acceptance is to compare the Z distribution for the data against the MC simulation. Figure 4 shows the vacuum-beam comparisons for the $\pi^+\pi^-$ and $\pi^0\pi^0$ signal modes as well as for the high statistics $\pi e \nu$ and

$3\pi^0$ samples. The overall agreement is quite good, but since the mean Z positions for K_L and K_S decays differ by about 6 m , a relative slope of 10^{-4} per meter in the data/MC ratio would cause an error of 10^{-4} on $\text{Re}(\epsilon'/\epsilon)$. As shown in Fig. 4 (b), the $\pi e\nu$ comparison agrees to better than this level; however, the $\pi^+\pi^-$ comparison has a slope of $(-1.60 \pm 0.63) \times 10^{-4}$ per meter. Although the significance of the $\pi^+\pi^-$ slope is marginal ($\sim 2.5\sigma$), we assign a systematic error on $\text{Re}(\epsilon'/\epsilon)$ based on the full size of the slope, 1.6×10^{-4} . The $3\pi^0$ and $\pi^0\pi^0$ Z distributions agree well, and we place a limit of 0.7×10^{-4} on the possible $\text{Re}(\epsilon'/\epsilon)$ bias from the neutral-mode acceptance.

Other checks on the acceptance include data/MC comparisons of track illuminations at the drift chambers and CsI, photon illumination at the CsI, and minimum photon separation distance. These all agree well and indicate no other sources of acceptance misunderstanding.

The final class of systematics includes possible differences in the K_S/K_L flux ratio between the $\pi^+\pi^-$ and $\pi^0\pi^0$ samples. The fact that using $\pi^+\pi^-$ and $\pi^0\pi^0$ data from different running periods is of little concern because the regenerator and movable absorber were the same for both periods; however, we assign a small uncertainty due to a possible temperature difference which might change their densities and thus the regenerator-beam attenuation. In addition, the $\pi^+\pi^-$ and $\pi^0\pi^0$ samples have somewhat different energy distributions, so the uncertainty in the energy dependence of the attenuation (measured using $\pi^+\pi^-\pi^0$ and $3\pi^0$ data) leads to a small uncertainty on $\text{Re}(\epsilon'/\epsilon)$.

Finally, we assign uncertainties corresponding to one-sigma variations of Δm and τ_S from the PDG averages,¹² and from a deviation of the phase of the regeneration amplitude by $\pm 0.5^\circ$ from the value given by analyticity.¹³ Adding all contributions in quadrature, the total systematic uncertainty on $\text{Re}(\epsilon'/\epsilon)$ is 2.8×10^{-4} .

We have performed several cross-checks on the $\text{Re}(\epsilon'/\epsilon)$ result. Consistent values are obtained at all kaon energies, and there is no significant variation as a function of time or beam intensity. Relaxing the power-law constraint on the regeneration amplitude yields a consistent value with the same precision.

We have also extracted $\text{Re}(\epsilon'/\epsilon)$ using an alternative fitting technique which compares the vacuum- and regenerator-beam Z distributions directly, eliminating the need for a Monte Carlo simulation to determine the acceptance. While statistically less powerful, this technique yields a value of $\text{Re}(\epsilon'/\epsilon)$ which is consistent with the standard analysis based on the uncorrelated parts of the statistical and systematic errors. In the end, using $\pi^+\pi^-$ data from 1996 (collected simultaneously with the $\pi^0\pi^0$ data) instead of from 1997 yields a consistent value of $\text{Re}(\epsilon'/\epsilon)$, 25×10^{-4} , allowing for a larger systematic error of 4×10^{-4} due to the 1996 Level 3 inefficiency.

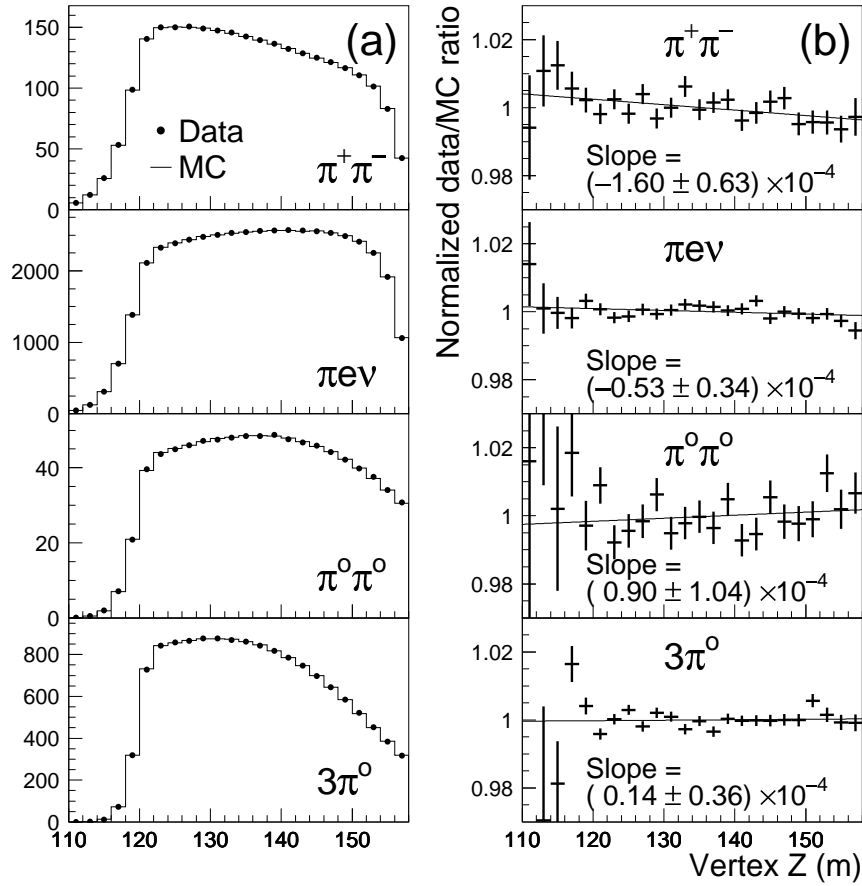


Figure 4: (a) Data versus Monte Carlo comparisons of vacuum-beam decay vertex Z distributions for $\pi^+\pi^-$, $\pi e\nu$, $\pi^0\pi^0$, and $3\pi^0$ decays. (b) Linear fits to the data/MC ratio of Z distributions for each of the four decay modes.

6 Conclusion

We have measured $\text{Re}(\epsilon'/\epsilon)$ to be $(28.0 \pm 3.0 \text{ (stat)} \pm 2.8 \text{ (syst)}) \times 10^{-4}$; combining the errors in quadrature, $\text{Re}(\epsilon'/\epsilon) = (28.0 \pm 4.1) \times 10^{-4}$. This result,¹⁴ nearly 7σ away from zero, firmly establishes the existence of CP violation in a “decay process”, agreeing better with the earlier measurement from NA31 than with E731,¹⁵ and shows that a superweak interaction cannot be the sole source of CP violation in the K meson system. The average of the three measurements (KTeV, NA31 and E731), $(21.7 \pm 3.0) \times 10^{-4}$, while at the high end of standard-model predictions, supports the notion of a nonzero phase in the CKM matrix. Further theoretical and experimental advances are needed before one can say whether or not there are other sources of CP violation beyond the standard model.

More data from KTeV are currently being processed through calibration and analysis to reduce both statistical and systematic uncertainties. At the same time, we are preparing to take more data again in 1999 with the aim of doubling the data statistics with much improved detector performance and additional systematic checks. We expect to reduce the $\text{Re}(\epsilon'/\epsilon)$ statistical uncertainty to $\sim 1 \times 10^{-4}$ and lower the systematics to a similar level.

References

1. J.H. Christenson, J.W. Cronin, V.L. Fitch and R. Turlay, *Phys. Rev. Lett.* **13**, 138 (1964).
2. B. Winstein and L. Wolfenstein, *Rev. Mod. Phys.* **65**, 1113 (1993).
3. M. Kobayashi and T. Maskawa, *Prog. Theo. Phys.* **49**, 652 (1973).
4. M. Ciuchini, *Nucl. Phys. Proc. Suppl.* **59**, 149 (1997).
5. A.J. Buras in *Probing the Standard Model of Particle Interactions*, ed. R. Gupta *et al.* (Elsevier, 1999); hep-ph/9806471.
6. S. Bertolini *et al.*, *Nucl. Phys. B* **514**, 93 (1998).
7. L. Wolfenstein, *Phys. Rev. Lett.* **13**, 569 (1964).
8. L. K. Gibbons *et al.*, *Phys. Rev. Lett.* **70**, 1203 (1993).
9. G. D. Barr *et al.*, *Phys. Lett. B* **317**, 233 (1993).
10. L. K. Gibbons *et al.*, *Phys. Rev. D* **55**, 6625 (1997).
11. H. Burkhardt *et al.*, *Nucl. Instrum. Methods A* **268**, 116 (1988).
12. Particle Data Group, C. Caso *et al.* *Eur. Phys. J. C* **3**, 1 (1998).
13. See R.A. Briere and B. Winstein, *Phys. Rev. Lett.* **75**, 402 (1995).
14. After the preliminary announcement, the final result has now been published in A. Alavi-Harati *et al.*, *Phys. Rev. Lett.* **83**, 22 (1999).
15. Scrutiny of E731 analysis has not revealed any explanation for its 2.9σ lower value other than a possible, if improbable, fluctuation.